GEOLOGICAL SURVEY OF CANADA
OPEN FILE 6827

An Assessment of a Potential Source of Industrial Limestone on Southampton Island, Nunavut

S. Zhang
E.C. Prosh
D.T. James

2011

Natural Resources Canada
Ressources naturelles Canada

Canada

GEOLOGICAL SURVEY OF CANADA
OPEN FILE 6827

An Assessment of a Potential Source of Industrial Limestone on Southampton Island, Nunavut

S. Zhang, E.C. Prosh, D.T. James

2011

©Her Majesty the Queen in Right of Canada 2011

doi:10.4095/288201

This publication is available from the Geological Survey of Canada Bookstore (http://gsc.nrcan.gc.ca/bookstore_e.php).
It can also be downloaded free of charge from GeoPub (http://geopub.nrcan.gc.ca/).

Recommended citation:
Zhang, S., Prosh, E.C., and James, D.T., 2011. An Assessment of a Potential Source of Industrial Limestone on Southampton Island, Nunavut. Open File 6827, 30p. doi:10.4095/288201

Publications in this series have not been edited; they are released as submitted by the author.

TABLE OF CONTENTS

1. Introduction……..……..….…..1

2. Regional Paleozoic Stratigraphy ……..……1

(1) Bad Cache Rapids Group…….…2
(2) Churchill River Group…….……3
(3) Red Head rapids Formation…….....3
(4) Severn River Formation…….……..4
(5) Ekwan River/Attawapiskat Formation…….....4

3. Sample Site Selection and locations ……..…….....4

(1) Site 1: Rocky Brook…….....4
(2) Site 2: Costal area east of Rocky Brook……..5
(3) Site 3: Fossil Creek……..5
(4) Site 4: east of Post River……..…5

4. Sample Methodology in the Field……...……....6

5. Whole Rock Geochemical Analysis. ……..9

(1) X-ray Diffraction Analysis……..9
(2) X-ray Fluorescence Analysis……14
(3) Comparison of XRD and XRF data……...16

6. Petrographic Analysis……21

(1) Mineralogy……21
(2) Rock Fabric……27

7. Conclusions and Possible Subsequent Work……28

(1) Conclusions……28
(2) Possible Subsequent Work……29

Acknowledgements……....30

References……..30

APPENDIX

Figure 2. Topography map showing sampling localities

1. INTRODUCTION

Limestone, consisting principally of calcium carbonate ($CaCO_3$), has a diversity of uses. It is used in the iron and steel industry, chemical and mining industries, in cement and glass making, in production of filters and pigments, and for agricultural use. In the mining industry, industrial limestone (lime) can be used as a chemical reagent in the neutralization of acid. In particular, treated lime is used in the recovery of gold and silver in cyanide leaching processes to curtail the loss of cyanide, and for pH control.

In view of recent and projected growth of the mining industry in the Kivalliq Region of Nunavut, a local source of industrial lime may have potential to meet demands of industry and reduce transportation costs to mine operators. An industrial limestone operation would provide significant opportunities for economic development and local employment.

Areas around Coral Harbour, Southampton Island, Nunavut (Fig. 1), contain extensive exposures of Lower Paleozoic limestone which may be suitable for industrial use.

The primary objectives of this study are to:

1) Better understand the stratigraphic and geographic distribution of relatively pure limestone intervals within the Lower Paleozoic formations near Coral Harbour on Southampton Island.

2) Provide an assessment of limestone purity based on detailed geochemical (both mineral and chemical) and petrographic data.

3) Identify potential quarry locations based on thickness and lateral continuity, if the limestone can be used by industry.

This Open File is a report of a field- and laboratory-based study of Lower Paleozoic limestones on parts of southern Southampton Island and assesses their potential as a source of industrial limestone. Field work took place in the 2009 field season.

2. REGIONAL PALEOZOIC STRATIGRAPHY

Lower Paleozoic units on Southampton Island (Figs. 1 and 2) include the Upper Ordovician Bad Cache Rapids Group, Churchill River Group, Red Head Rapids Formation, and the Lower Silurian Severn River and Ekwan River/Attawapiskat formations (Heywood and Sanford, 1976). The rocks, distributed in the southern and western parts of Southampton Island (Figs. 1 and 2), are flat lying, undeformed and unmetamorphosed. Typically, the Lower Paleozoic rocks are exposed as broad areas of sub-cropping rubble, although layered outcrops are commonly found along rivers and creeks.

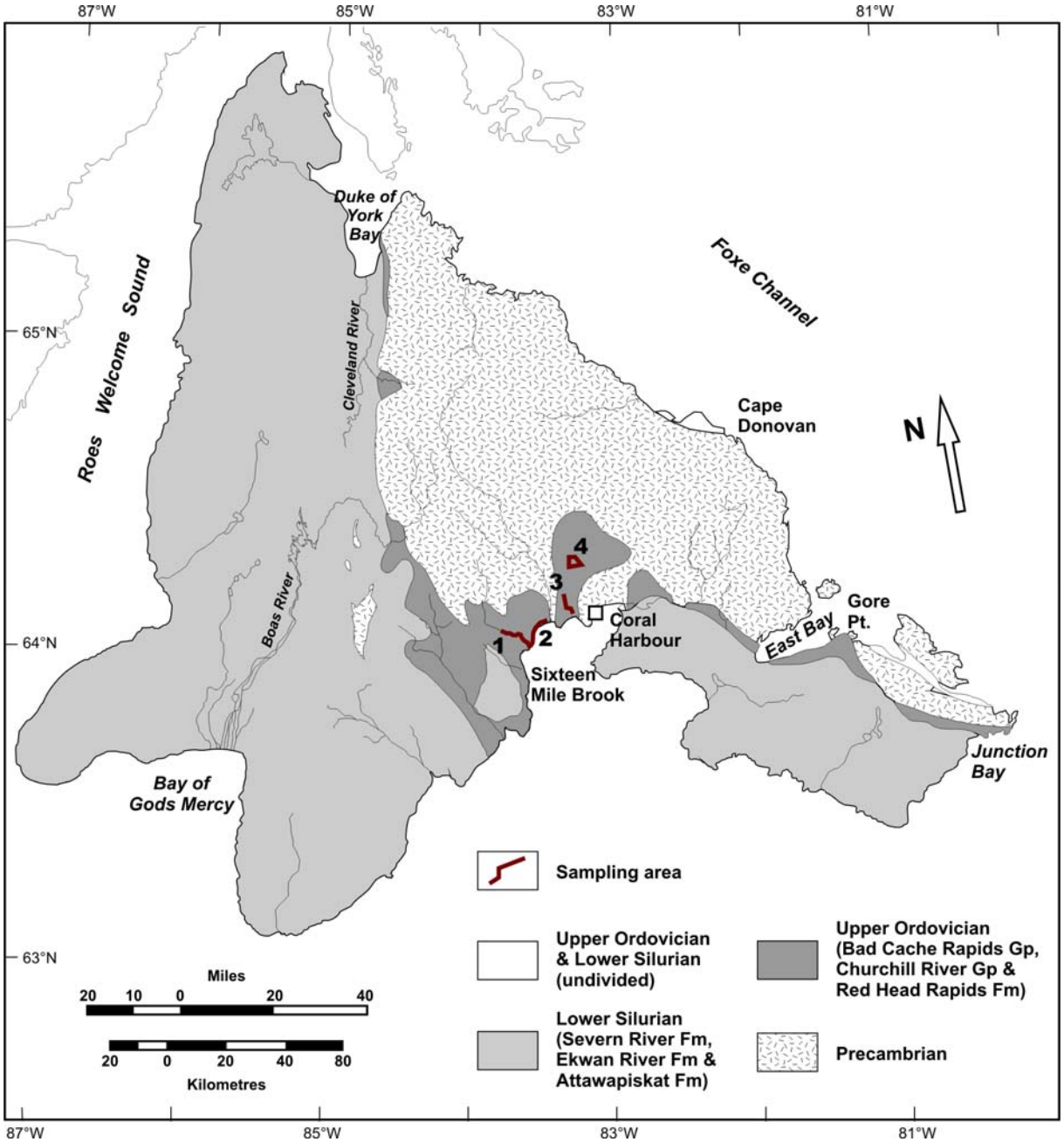

Figure 1. Simplified geological map of Southampton Island with site locations (modified from Heywood and Sanford, 1976, and Zhang, 2008; see Fig. 2 for detailed sample location). Red lines and polygon represent four sample locations: 1) Rocky Brook; 2) Coastal area east of Rocky Brook; 3) Fossil Creek; 4) East of Post River.

(1) Bad Cache Rapids Group

The Bad Cache Rapids Group unconformably overlies the Precambrian crystalline basement. It is a dark-grey or brown-grey fossiliferous limestone with a thin layer (about 1-2 m) of basal sandstone. It is characterized by yellowish orange irregular zones of mottling on almost all bedding planes (Fig. 3). The limestone contains abundant corals,

gastropods, nautiloids, algae, crinoids and trace fossils. On Southampton Island, the group has a maximum thickness of approximately 65 m (Zhang, 2011).

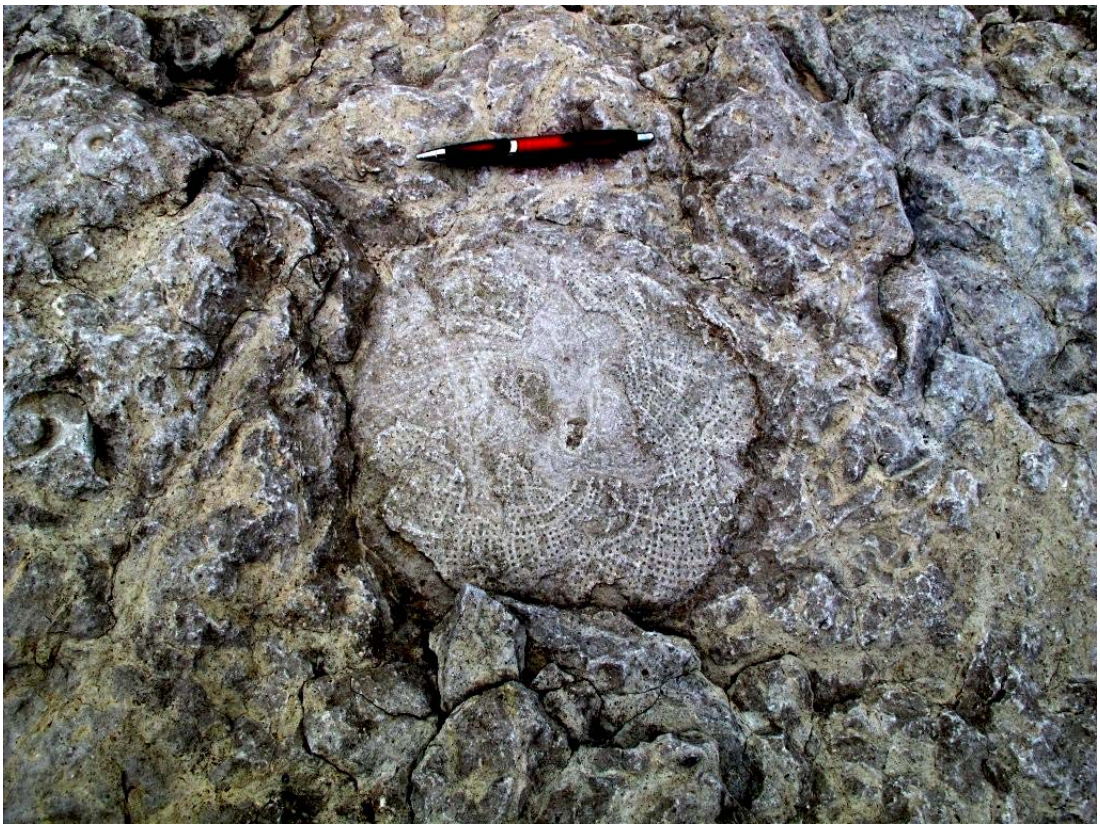

Figure 3. Typical lithology of the Bad Cache Rapids Group – limestone containing yellowish orange irregular zones of mottling on the bedding plane and abundant macrofossils (note the algae in the middle and gastropods on the left).

(2) Churchill River Group

The Churchill River Group conformably overlies the Bad Cache Rapids Group (Zhang, 2011). It consists of greenish grey- or gray-brown argillaceous dolomitic limestone. It is distinguished from the Bad Cache Rapids Group rocks by its dark greenish-grey weathered colour, argillaceous character, lack of macrofossils and yellowish orange irregular zones of mottling on the bedding planes. The lower Churchill River Group is more easily eroded than the Bad Cache Rapids Group and commonly forms a "stair-step" topography consisting of benches near the contact between the two groups. The maximum thickness of the formation is undetermined on Southampton Island.

(3) Red Head Rapids Formation

The Red Head Rapids Formation conformably overlies the Churchill River Group; the contact between these two units is transitional. The Red Head Rapids Formation has a distinctive orange-tan colour, and is mostly composed of dolostone, and is in striking contrast to the grey limestone-dominated Bad Cache Rapids and Churchill River groups. The Red Head Rapids Formation is divided into laminated beds (unit 1), breccia beds

(unit 2), biostromal beds (unit 3), and biohermal beds (unit 4) (Zhang, 2008). The maximum thickness of the formation is greater than 61 m on Southampton Island (Zhang, 2011).

(4) Severn River Formation

The Severn River Formation disconformably overlies the Red Head Rapids Formation. It consists primarily of brown microcrystalline limestone and dolostone; at a number of localities, Severn River strata have been intensely dolomitized (Sanford in Heywood and Sanford, 1976). The thickness of the formation on Southampton Island is unknown.

(5) Ekwan River/Attawapiskat Formation

The Ekwan River Formation conformably overlies the Severn River Formation. By contrast, work by Suchy and Stearn (1992) suggests that a disconformity exists between the units in the Hudson Bay Basin. The Ekwan River Formation consists of well-bedded, skeletal and pelletoidal limestone and fine-grained dolostone. The upper part of the formation passes laterally into the Attawapiskat Formation consisting of a reef-bearing carbonate unit with algal and stromatoporoid bioherms.

The three Upper Ordovician units (Bad Cache Rapids and Churchill River groups and Red Head Rapids Formation) are correlative to the upper Edenian–lowest Richmondian Stage (Zhang and Barnes, 2007; Zhang, 2011); and the three Lower Silurian units (Severn River, Ekwan River/Attawapiskat formations) to the Llandovery Stage (Zhang and Barnes, 2007) based on conodont data.

3. Sample Site Selection and Locations

Sampling was stratigraphically targeted to the Bad Cache Rapids Group and lower Churchill River Group, which was based on prior field observation made by the primary author (Zhang, 2008). These units contain relatively pure limestone compared to other units (e.g. less dolomite) within the Upper Ordovician succession on Southampton Island. The sampling was geographically restricted to areas close to Coral Harbour, based on the best exposures of Bad Cache Rapids Group and lower Churchill River Group limestones, and the thickness of accessible sections. These areas are accessible by vehicle or ATV, via gravel road or hunting trails.

Four major areas (Fig. 1) near Coral Harbour were chosen for sampling, which include Rocky Brook (localities 06–12 in Fig. 2), the coastal area east of Rocky Brook (localities 13–17 in Fig. 2), Fossil Creek (localities 01–05 in Fig. 2) and east of Post River (localities 18–21 in Fig. 2).

(1) Site 1: Rocky Brook

The mouth of Rocky Brook is located ca. 30 km west of Coral Harbour; samples were collected at localities 06 to 12 (Figs. 1 and 2; see Table 1 for coordinates). The site contains exposures of the Bad Cache Rapids Group.

At locality 22, Bad Cache Rapids Group limestone unconformably overlies Precambrian metamorphic granite. At locality 06 (Fig. 2), the unconformity is exposed again (Fig. 4A). The entire Bad Cache Rapids Group is intermittently exposed along Rocky Brook from locality 22 to locality 12 (Fig. 4B and 4C). Exposure of the Bad Cache Rapid Group ends at locality 12, where the boundary between Bad Cache Rapids and Churchill River groups is well exposed (Fig. 4D). A composite section from locality 06 to locality 12 should include the entire Bad Cache Rapids Group, although exposure is not continuous. Within this interval, samples were collected at 7 localities (locality 06 to locality 12) (Table 1).

The thickness of the Bad Cache Rapids Group along Rocky Brook is imprecisely known, although a continuous section of the Bad Cache Rapids Group in the Duke of York Bay area was measured at about 65 m (Zhang, 2011).

(2) Site 2: Coastal area east of Rocky Brook

Site 2 (Fig. 1) includes a large coastal area east of Rocky Brook. It covers locality 12 where the lowest Churchill River Group is exposed (Fig. 4D); from locality 12 east towards locality 15 (Fig. 2), the lower Churchill River Group forms a cliff parallel to the coast. Between the cliff and shore line, a huge area is covered by wave-washed limestone rubble (Fig. 4H). The samples at localities 13 and 14 are from the cliff, and those at localities 16 and 17 are from rubble (See Table 1 for coordinates). The rubble samples may contain rocks from both Bad Cache Rapids and Churchill River groups.

(3) Site 3: Fossil Creek

Site 3 includes Fossil Creek and its surrounding area (Figs. 1 and 2). The rocks exposed along Fossil Creek are correlated to middle–upper Bad Cache Rapids Group based on conodont data (Zhang, 2011). Samples from localities 01 (Fig. 4E) and 02 are from outcrops along Fossil Creek from the bridge piers to the north where the outcrop pinches out, extending about 300 meters. Samples from localities 03–05 are from both piled road-building material and outcrop on the ground of the local shallow quarries (Fig. 4G) (See Table 1 for coordinates).

The exposed Bad Cache Rapids Group along Fossil Creek is approximately 8–9 m thick.

(4) Site 4: East of Post River

The plateau east of the Post River area and ca. 15–20 km north of Coral Harbour is composed of limestone of the Bad Cache Rapids Group. Samples from locality 21 were collected from the base of the Bad Cache Rapids Group limestone immediately above the basal sandstone; the samples from localities 19 and 20 are stratigraphically higher than that from locality 21. Based on the contour lines in this area and the near-horizontal strata, this plateau most likely contains the entire Bad Cache Rapids Group and the lower Churchill River Group. All the samples from localities 18–21 are from outcrops exposed along south-draining creeks (e.g. Fig. 4F) (See Table 1 for coordinates).

4. Sample Methodology in the Field

A total of 22 localities were examined, of which 20 localities were sampled. A total of 44 samples were collected for geochemical analyses, of which 41 and 3 were from outcrop and rubble, respectively. For whole rock X-ray Diffraction (XRD) and X-ray Fluorescence (XRF) analyses, chip samples were carefully collected from outcrop along the rivers, creeks and cliffs. In the continuous sections, all the sample intervals are ≤ 1.5 m. Within the 1.5 m interval, chips with as uniform size as possible were taken at equal spacing across the 1.5 m interval. Weathered surfaces were avoided where possible, and the weathered rind on the chip samples was discarded.

A total of 39 hand samples were collected from outcrop for petrographic study, within the 1.5 m intervals that were chip-sampled.

All the stratigraphic and geographic locations, sample field and GSC numbers, and sample types are summarized in Table 1.

Table 1. Samples, sample stratigraphic and geographic locations, and sample type

Location	Stratigraphy	station ID	Latitude	Longitude	Geochemistry Samples		Petrography Samples		Sample Type
					field ID	GSC ID	field ID	GSC ID	
Fossil Creek & nearby area	mid-upper Bad Cache Rapids Gp	01	64°10′47.0″N	83°21′30.1″W	09SZ-01-01G	O-203574	09SZ-01-01TS	O-203578	outcrop
					09SZ-01-02G	O-203575	09SZ-01-02TS	O-203579	outcrop
		02	64°10′45.1″N	83°21′20.5″W	09SZ-02-01G	O-203580	09SZ-02-01TS	O-203584	outcrop
					09SZ-02-02G	O-203581	09SZ-02-02TS	O-203585	outcrop
		03	64°08′36.8″N	83°16′11.3″W	09SZ-03-01G	O-203586	09SZ-03-01TS	O-203590	outcrop
		04	64°08′41.3″N	83°18′11.5″W	09SZ-04-01G	O-203591			rubble
					09SZ-04-02G	O-203592	09SZ-04-02TS	O-203595	outcrop
		05	64°08′51.1″N	83°16′29.9″W	09SZ-05-01G	O-203596			outcrop
Rocky Brook	lower Bad Cache Rapids Gp	06	64°04′56.5″N	83°45′07.9″W	09SZ-06-01G	O-203598	09SZ-06-01TS	O-203604	outcrop
					09SZ-06-02G	O-203599	09SZ-06-02TS	O-203605	outcrop
					09SZ-06-03G	O-203600	09SZ-06-03TS	O-203606	outcrop
	Bad Cache Rapids Gp	07	64°05′02.0″N	83°44′07.3″W	09SZ-07-01G	O-203607	09SZ-07-01TS	O-203617	outcrop
					09SZ-07-02G	O-203608	09SZ-07-02TS	O-203618	outcrop
					09SZ-07-03G	O-203609	09SZ-07-03TS	O-203619	outcrop
					09SZ-07-04G	O-203610	09SZ-07-04TS	O-203620	outcrop
					09SZ-07-05G	O-203611	09SZ-07-05TS	O-203621	outcrop
		08	64°04′39.7″N	83°42′26.3″W	09SZ-08-01G	O-203622	09SZ-08-01TS	O-203624	outcrop
		09	64°03′31.5″N	83°38′43.0″W	09SZ-09-01G	O-203625	09SZ-09-01TS	O-203633	outcrop
					09SZ-09-02G	O-203626	09SZ-09-02TS	O-203634	outcrop
					09SZ-09-03G	O-203627	09SZ-09-03TS	O-203635	outcrop
					09SZ-09-04G	O-203628	09SZ-09-04TS	O-203636	outcrop
		10	64°03′04.6″N	83°37′49.8″W	09SZ-10-01G	O-203637	09SZ-10-01TS	O-203639	outcrop
	top B. C. R. Gp	11	64°02′46.2″N	83°36′35.0″W	09SZ-11-01G	O-203640	09SZ-11-01TS	O-203644	outcrop
					09SZ-11-02G	O-203641	09SZ-11-02TS	O-203645	outcrop
	base Churchill River Group	12	64°02′25.8″N	83°35′51.1″W	09SZ12-01G	O-203648	09SZ12-01TS	O-203652	outcrop
					09SZ12-02G	O-203649	09SZ12-02TS	O-203653	outcrop
					09SZ12-03G	O-205923			outcrop
Coastal area east of Rocky Brook	Churchill River Group	13	64°03′15.3″N	83°34′45.3″W	09SZ-13-01G	O-203654	09SZ-13-01TS	O-203658	outcrop
					09SZ-13-02G	O-203655	09SZ-13-02TS	O-203659	outcrop
		14	64°03′47.5″N	83°34′33.0″W	09SZ-14-01G	O-203661	09SZ-14-01TS	O-203665	outcrop
					09SZ-14-02G	O-203662	09SZ-14-02TS	O-203666	outcrop
		15	64°05′47.8″N	83°33′45.1″W	no sample				
	mixed B.C.R. & C.R.	16	64°04′28.0″N	83°33′56.7″W	09SZ-16-01G	O-203668			rubble
		17	64°02′52.6″N	83°34′46.7″W	09SZ-17-01G	O-203670			rubble
East of Post River	lower Bad Cache Rapids Gp	18	64°17′28.9″N	83°02′52.1″W	09SZ-18-01G	O-203672	09SZ-18-01TS	O-203678	outcrop
					09SZ-18-02G	O-203673	09SZ-18-02TS	O-203679	outcrop
					09SZ-18-03G	O-203674	09SZ-18-03TS	O-203680	outcrop
		19	64°18′36.5″N	83°05′10.9″W	09SZ-19-01G	O-203681	09SZ-19-01TS	O-203683	outcrop
		20	64°18′36.0″N	83°06′18.6″W	09SZ-20-01G	O-203684	09SZ-20-01TS	O-203696	outcrop
					09SZ-20-02G	O-203685	09SZ-20-02TS	O-203697	outcrop
					09SZ-20-03G	O-203686	09SZ-20-03TS	O-203698	outcrop
					09SZ-20-04G	O-203687	09SZ-20-04TS	O-203699	outcrop
					09SZ-20-05G	O-203688	09SZ-20-05TS	O-203700	outcrop
					09SZ-20-06G	O-203689	09SZ-20-06TS	O-203701	outcrop
		21	64°17′04.9″N	83°06′23.8″W	09SZ-21-01G	O-203705	09SZ-21-01TS	O-203707	outcrop
Rocky Brook		22	64°10′02.3″N	83°56′38.8″W	no sample				

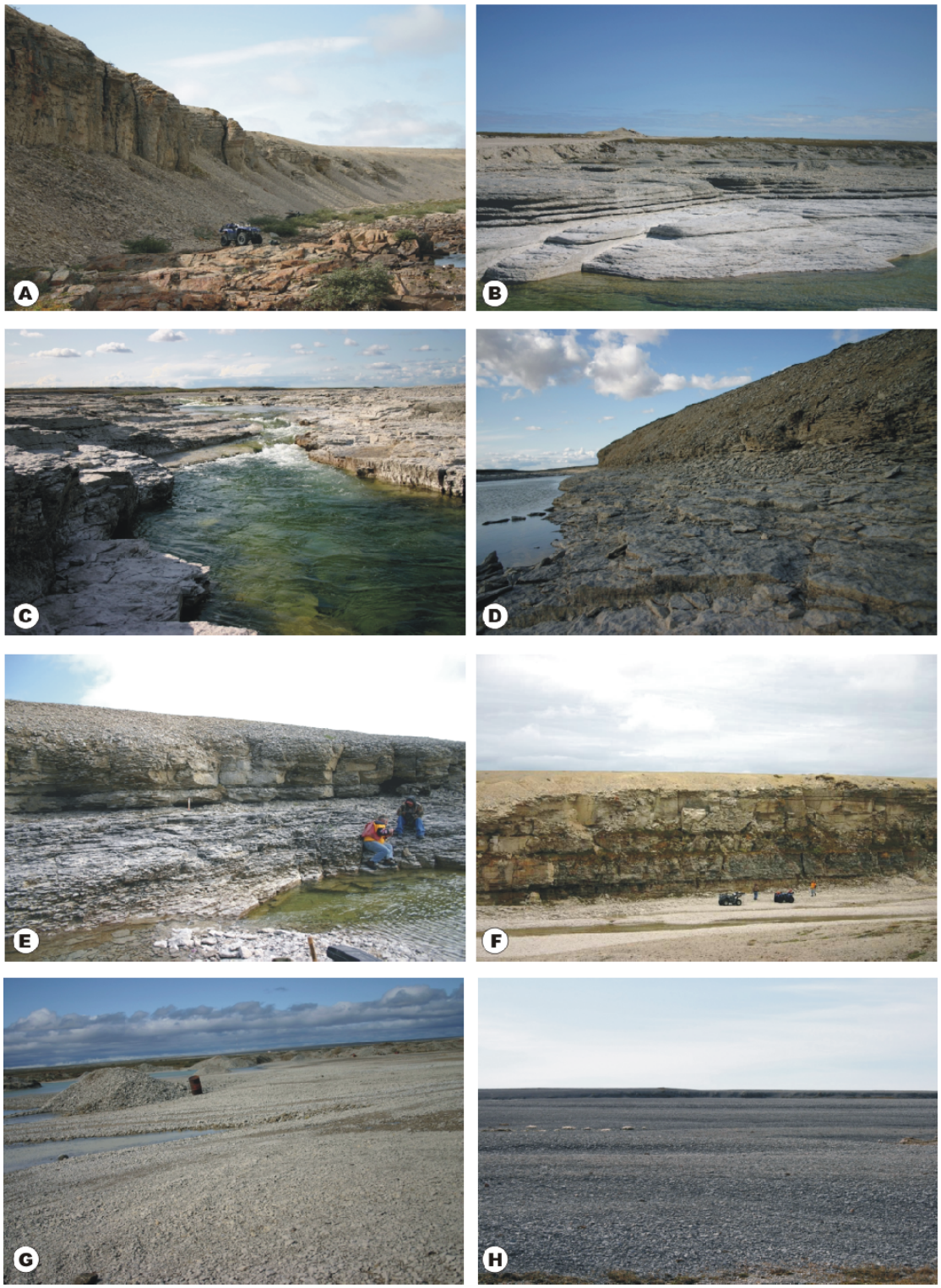

Figure 4. Outcrops of Bad Cache Rapids and lower Churchill River groups on Southampton Island. A. unconformity between Precambrian and Bad Cache Rapids Group at locality 06 along Rocky Brook; B and C. outcrops of Bad Cache Rapids Group at localities 09 and 11 along Rocky Brook; D. conformable contact between Bad Cache Rapids and Churchill River groups at locality 12 near the mouth of Rocky Brook; E. outcrop of Bad Cache Rapids Group at locality 01 along Fossil Creek; F. outcrop of lower Bad Cache Rapids Group at locality 21 in the east of Post River; G. Bad Cache Rapids Group is exposed in a quarry at locality 03 near Coral Harbor; H. huge area covered by limestone rubble at locality 13 along the coast east of Rocky Brook.

5. WHOLE ROCK GEOCHEMICAL ANALYSIS

Both mineralogical and chemical methods were employed to collect geochemical data. X-ray Diffraction (XRD) analysis was performed for identification and quantification of major and minor minerals, and both X-ray Fluorescence (XRF) and Total Sulphur and Carbon analyses for determination of major and minor oxides and several trace elements. These analyses (44 samples) were performed by the Analytical Chemistry Laboratories of the Geological Survey of Canada (GSC), Ottawa.

(1) X-ray Diffraction Analysis

The following methodology and results were provided by Igor Bilot and Jeanne B. Percival (Analytical Chemistry Laboratories, GSC).

1) Methodology

The mineralogy of whole rock samples was determined by X-ray powder diffraction analysis (XRD). X-ray patterns of the pressed powder samples were recorded on a Bruker D8 Advance Powder Diffractometer equipped with a graphite monochromator, using Co Kα radiation with X-ray tube settings of 40 kV and 40 mA. X-ray patterns were captured digitally and the raw data files were processed using Bruker software, including EVA and TOPAS. EVA allows pattern smoothing, background removal and peak identification and is mainly used as a Search/Match tool to identify mineral phases. Once minerals were identified, quantification using Rietveld refinement was performed using TOPAS, a graphics-based profile analysis program based on non-linear least squares fitting (Bruker, 2008). TOPAS relies on fitting the mineral phases with crystal structure models available from published (e.g., Pearson's Crystal Database; International Centre of Diffraction Data (ICDD)) and on-line (e.g., American Mineralogist) databases. The structure fitted to a particular unknown phase is a best fit, not necessarily a perfect fit. Percent error was not calculated; it is assumed to be < 5 wt%.

2) Results

All samples are dominated by calcite (Table 2). Minor quartz (2-6 wt%), dolomite (2- 12 wt%) and slight traces of chlorite and mica occur. Figure 5 shows a typical XRD trace of the samples where calcite is identified by its strong 3.03 Å X-ray peak, dolomite by its 2.88 Å peak and quartz by the 4.26 and 3.34 Å peaks. Chlorite was identified by the presence of a very small 14 Å X-ray peak, and mica by a 10 Å peak.

In TOPAS, both dolomite and ankerite crystal structures fit the XRD trace. Analyses using the Scanning Electron Microscope (SEM) were used to determine if Fe was present (as no XRF data were available at the time). As no Fe was detectable in samples 09SZ-01-01, 09SZ-03-01, 09SZ-09-04 and 09SZ-12-03, it was assumed that the second carbonate phase was dolomite (Fig. 6).

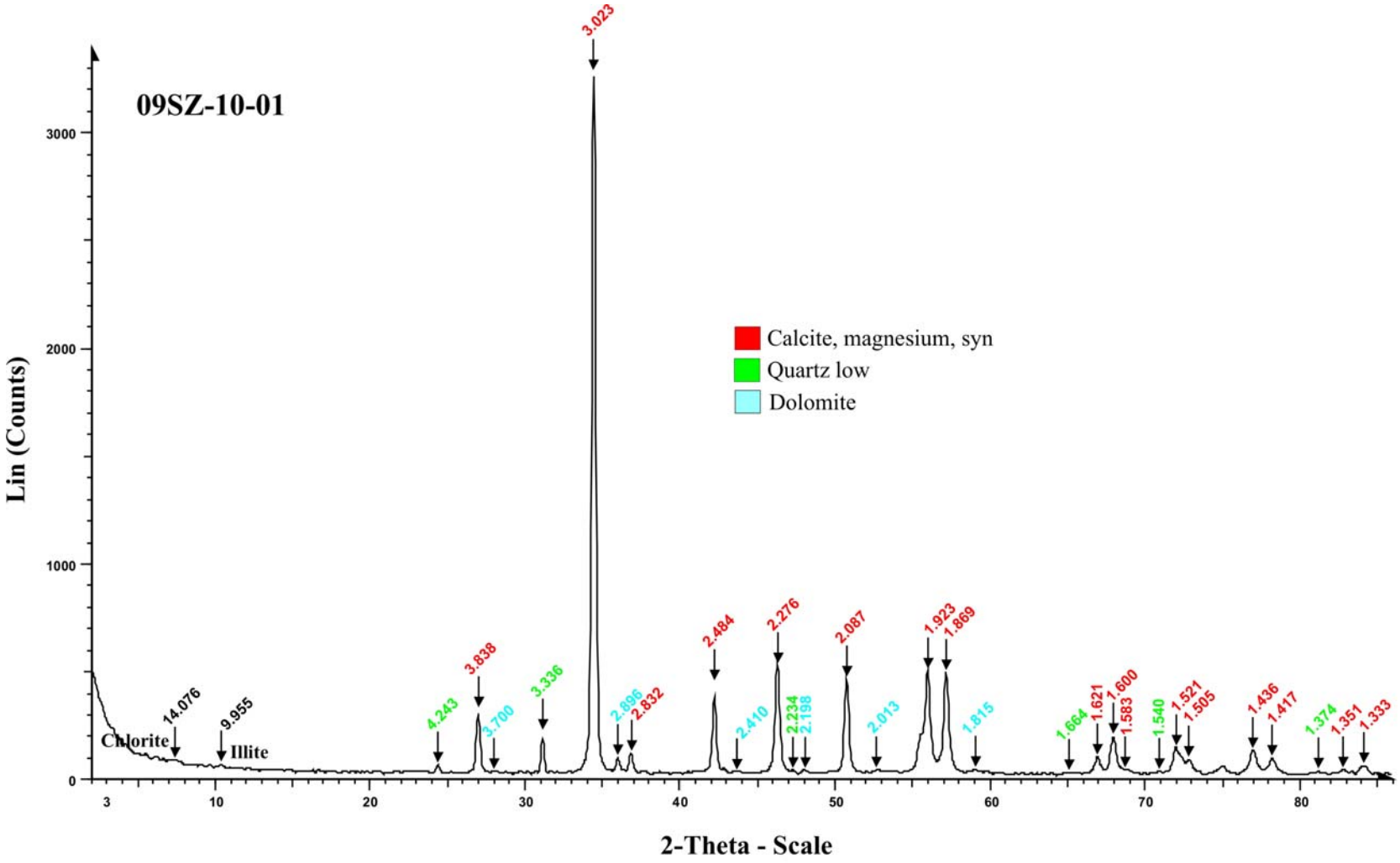

Figure 5. XRD trace of sample 09SZ-10-01 with trace illite and chlorite in addition to major minerals quartz, calcite and dolomite.

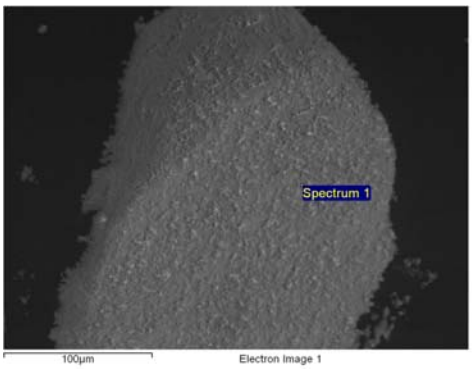

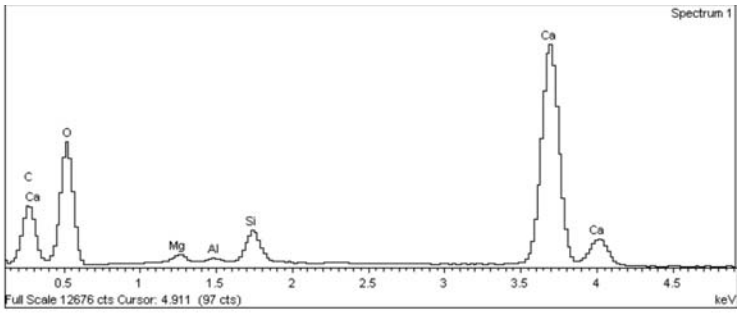

A: EDS spectra of sample 09-SZ-01-01

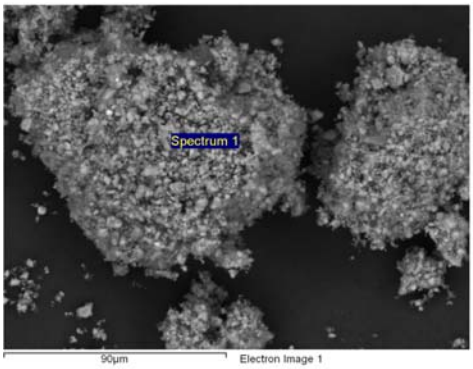

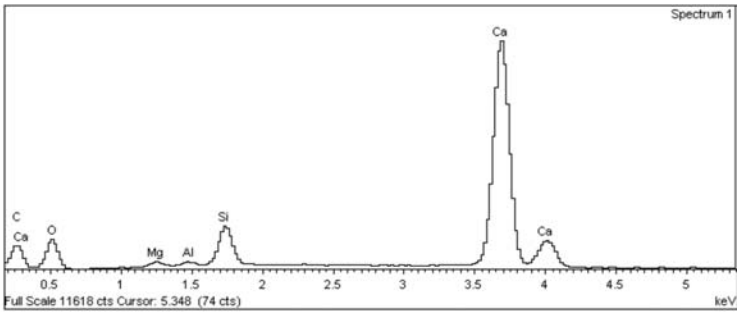

B: EDS spectra of sample 09-SZ-03-01

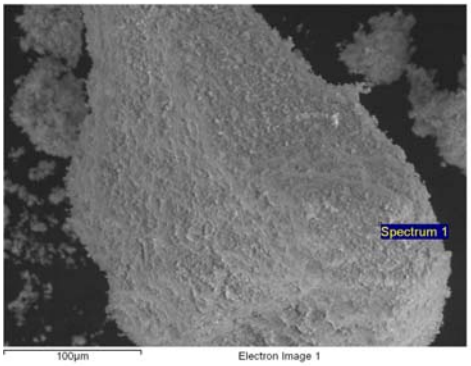

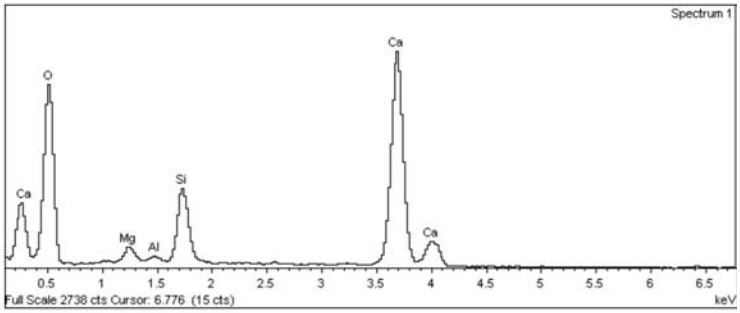

C: EDS spectra of sample 09-SZ-09-04

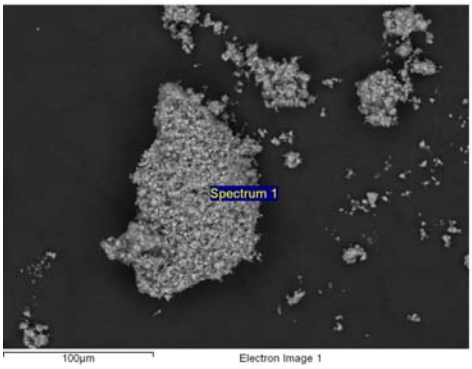

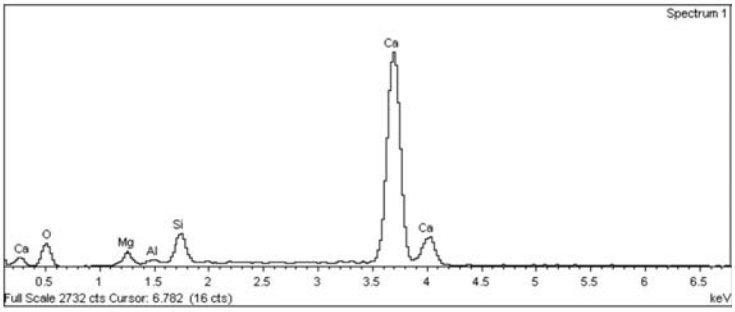

D: EDS spectra of sample 09-SZ-12-03

Figure 6. EDS spectra of four samples

Table 2. Quantitative mineralogy of whole rock samples by XRD and rietveld refinement

Samples	Calcite	Quartz	Dolomite
	wt %	wt %	wt %
09SZ-01-01	95.2	2.7	2.1
09SZ-01-02	93.6	3	3.4
09SZ-02-01	93.4	2.7	3.9
09SZ-02-02	91.5	3	5.5
09SZ-03-01	94.6	2.5	2.7
09SZ-04-01	94.1	3	3
09SZ-04-02	93.3	2.7	4
09SZ-05-01	93.4	2.8	3.8
09SZ-06-01	93.9	3	3.2
09SZ-06-02	92.9	3.1	4
09SZ-06-03	94.2	2.8	3
09SZ-07-01	96.6	3.1	0.2
09SZ-07-02	96.2	3.1	0.8
09SZ-07-03	95	3	2
09SZ-07-04	95.5	3.1	1.4
09SZ-07-05	96.3	2.5	1
09SZ-08-01	91.8	3.4	4.6
09SZ-09-01	95.7	2.5	1.8
09SZ-09-02	91.1	3.6	5.3
09SZ-09-03	91.4	2.8	5.8
09SZ-09-04	84.8	3.6	11.5
09SZ-10-01	90.9	3.1	6
09SZ-11-01	87.9	4	8.1
09SZ-11-02	87.8	3.2	9
09SZ12-01	87.4	3.3	9.3
09SZ12-02	86.6	3.3	10.2
09SZ12-03	84.6	3.4	11.9
09SZ-13-01	96.8	2.3	0.9
09SZ-13-02	98	1.2	0.7
09SZ-14-01	85.4	6.2	8.4
09SZ-14-02	90.6	4.8	4.6
09SZ-16-01	96.3	3.3	0.4
09SZ-17-01	91	2.7	6.2
09SZ-18-01	94.4	3	2.6
09SZ-18-02	93.6	3.2	3.3
09SZ-18-03	94	2.5	3.5
09SZ-19-01	93.8	2.4	3.8
09SZ-20-01	94.7	3.2	2
09SZ-20-02	92.5	3.3	4.2
09SZ-20-03	90.3	3.3	6.3
09SZ-20-04	92.7	2.9	4.3
09SZ-20-05	92.6	3.3	4.1
09SZ-20-06	93.7	3.1	3.2
09SZ-21-01	88.1	2.8	9.1

Note: 1) All samples contain slight traces of chlorite and mica. Sample 09-SZ-01-01 and 03-01 (2-3 wt% dolomite) and samples 09-SZ-09-04 and 12-03 (~ 10 wt% dolomite) have been analysed for iron content by SEM-EDS and no ankerite was observed.
2) See Table 1 for samples' stratigraphic and geographic information.

3) Classification of limestone by purity

Based on the British Geological Survey scheme for the classification of limestone by purity (after Harrison, 1993), and the XRD data in Table 2, the purity of most limestone samples from the Bad Cache Rapids and lower Churchill River groups on Southampton Island can be classified as low–medium. Of 44 samples collected, 1 can be classified as high purity (98.5–97% $CaCO_3$), 20 medium purity (97–93.5% $CaCO_3$), 21 low purity (93.5–85% $CaCO_3$) and 2 impure (<85% $CaCO_3$) (Table 3; Fig. 7). The samples with <90% calcite are concentrated in the boundary interval between the Bad Cache Rapids and Churchill River groups, and the lowest limestone interval of the Bad Cache Rapids Group right above the basal sandstone.

Table 3. Classification of limestone by purity (after Harrison, 1993) and grade of limestone on Southampton Island based on data ($CaCO_3$) collected by XRD

No	Percentage of		Category	Limestone on Southampton Island (number of samples)
	$CaCO_3$	Equivalent CaO		
1	> 98.5	> 55.2	Very high purity	0% (0/44)
2	98.5 - 97.0	55.2 - 54.3	High purity	2.3% (1/44)
3	97.0 - 93.5	54.3 - 52.4	Medium purity	45.5% (20/44)
4	93.5 - 85.0	52.4 - 47.6	Low purity	47.7% (21/44)
5	< 85.0	< 47.6	Impure	4.6% (2/44)

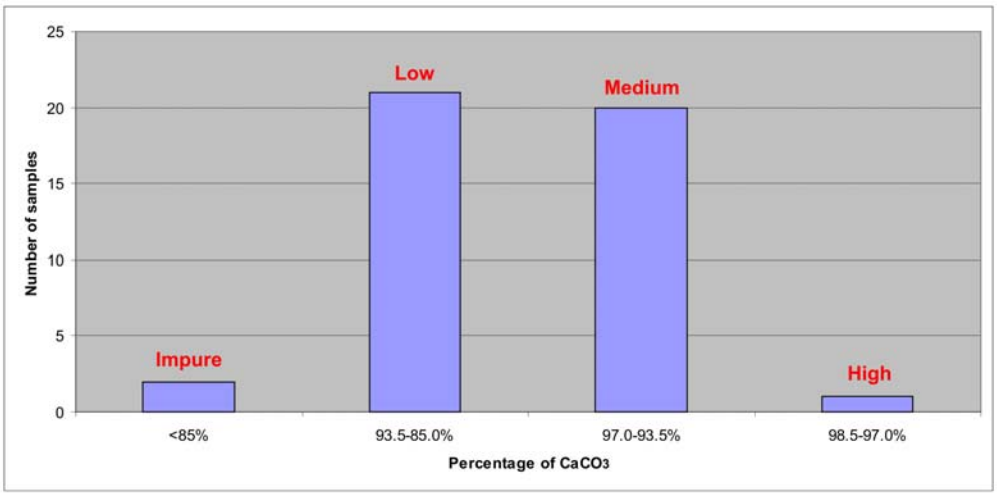

Figure 7. Classification of limestone by purity (after Harrison, 1993) on Southampton Island based on XRD data ($CaCO_3$)

(2) X-ray Fluorescence Analysis

1) Methodology

Major (except S and C) and trace element concentrations were determined by X-ray fluorescence (XRF) spectrometry. XRF is widely used for bulk analysis of major and minor elements in geological matrices (rocks, minerals, and sediment). The instrument used was a PANalytical Axios wavelength-dispersive spectrometer.

The determination limits and precision estimates of XRF for all major and trace elements are summarized in Table 4, which is more precise than XRD (5%).

Table 4. Determination Limits and Precision Estimates (Analytical Chemistry Laboratories, Central Canada Division, GSC).

	XRF-Fused Disk Major Elements		
	Determination limit (wt %)	Precision*	
		Absolute (wt %)	Relative (% of concn.)
SiO_2	0.4	0.4	1
TiO_2	0.05	0.05	1
Al_2O_3	0.2	0.2	1
Cr_2O_3	0.02	0.02	1
Fe_2O_3T	0.1	0.1	1
MnO	0.02	0.02	1
MgO	0.1	0.1	1
CaO	0.1	0.1	1
Na_2O	0.1	0.1	1
K_2O	0.05	0.05	1
P_2O_5	0.02	0.02	1
S**	0.02	0.02	5

	XRF-Fused Disk Trace Elements		
	Determination limit (ppm)	Precision*	
		Absolute (ppm)	Relative (% of concn.)
Ba	30	30	3
Nb	20	20	3
Rb	20	20	2
Sr	20	20	2
Zr	20	20	2

* Precision – the larger of the two measures, absolute or relative, applies

** S by combustion/ infra-red spectrometry

2) Results

All samples are dominated by calcium oxide (CaO, 53.56–44.73%), with minor silicon dioxide (SiO_2, 9.9–2.0%) and magnesium oxide (MgO, 3.53–0.95%). Alumina (Al_2O_3, 2.5–0.5%) and iron (III) oxide (Fe_2O_3, 0.8–03%) (some of the iron may be as pyrite) also contribute a small proportion of the whole rock. Of the trace elements, Ba, Nb, Rb, Sr and Zr, only Sr (strontium) was detected consistently (Table 5).

Table 5. Results of Chemical Analysis by XRF

Sample Field ID	SiO_2	TiO_2	Al_2O_3	Cr_2O_3	Fe_2O_3T	MnO	MgO	CaO	Na_2O	K_2O	P_2O_5	Ba	Nb	Rb	Sr	Zr	ST	CO_2T	LOI	TOTAL
	Wt%	Wt%	Wt%	Wt%	Wt%	Wt%	Wt%	Wt%	Wt%	Wt%	Wt%	ppm	ppm	ppm	ppm	ppm	Wt%	Wt%	Wt%	Wt%
09SZ-01-01G	4.0	<0.05	0.6	<0.02	0.3	<0.02	1.75	51.61	<0.1	<0.05	<0.02	<30	<20	<20	261	<20	0.08	41.8	41.7	100.1
09SZ-01-02G	4.3	<0.05	0.7	<0.02	0.3	<0.02	2.00	50.45	<0.1	<0.05	<0.02	<30	<20	<20	261	<20	0.05	41.8	41.6	99.5
09SZ-02-01G	4.3	<0.05	0.7	<0.02	0.4	<0.02	2.14	50.55	<0.1	0.05	<0.02	<30	<20	<20	256	<20	0.07	42.0	41.5	99.7
09SZ-02-02G	4.2	<0.05	0.8	<0.02	0.4	<0.02	2.51	50.15	<0.1	0.07	<0.02	<30	<20	<20	287	57	0.03	41.7	41.6	99.7
09SZ-03-01G	3.7	<0.05	0.6	<0.02	0.3	0.02	1.86	51.39	<0.1	<0.05	<0.02	<30	<20	<20	267	<20	0.07	42.0	41.8	99.8
09SZ-03-02G	4.3	<0.05	0.6	<0.02	0.3	0.02	2.17	50.63	<0.1	<0.05	<0.02	<30	<20	<20	266	<20	0.10	41.7	41.5	99.7
09SZ-04-01G	4.5	<0.05	0.7	<0.02	0.4	0.02	1.99	50.83	<0.1	0.08	<0.02	<30	<20	<20	252	<20	0.10	41.5	41.2	99.7
09SZ-04-02G	3.8	<0.05	0.6	<0.02	0.3	0.02	1.81	51.39	<0.1	<0.05	<0.02	<30	<20	<20	255	<20	0.09	42.0	41.7	99.7
09SZ-05-01G	4.2	<0.05	0.7	<0.02	0.4	<0.02	2.14	50.25	<0.1	<0.05	<0.02	<30	<20	<20	255	<20	0.10	41.6	41.4	99.2
09SZ-06-01G	4.4	<0.05	0.7	<0.02	0.4	<0.02	2.04	50.71	<0.1	<0.05	<0.02	<30	<20	<20	257	<20	0.06	41.4	41.4	99.7
09SZ-06-02G	4.6	<0.05	0.7	<0.02	0.4	<0.02	2.18	50.54	<0.1	<0.05	<0.02	<30	<20	<20	264	<20	0.06	41.3	41.4	99.9
09SZ-06-03G	4.1	<0.05	0.6	<0.02	0.3	<0.02	1.92	50.98	<0.1	<0.05	<0.02	<30	<20	<20	261	<20	0.04	42.8	41.7	99.7
09SZ-07-01G	4.4	<0.05	0.7	<0.02	0.4	0.02	1.38	51.55	<0.1	<0.05	<0.02	<30	<20	<20	271	<20	0.06	42.3	41.4	99.9
09SZ-07-02G	4.4	<0.05	0.7	<0.02	0.4	<0.02	1.50	50.82	<0.1	<0.05	<0.02	<30	<20	<20	260	<20	0.06	42.5	41.3	99.3
09SZ-07-03G	4.5	<0.05	0.8	<0.02	0.4	<0.02	1.76	50.98	<0.1	0.05	<0.02	<30	<20	<20	256	<20	0.05	41.9	41.4	99.8
09SZ-07-04G	4.3	<0.05	0.7	<0.02	0.3	<0.02	1.55	51.78	<0.1	0.07	<0.02	<30	<20	<20	258	<20	0.04	42.2	41.2	100.0
09SZ-07-05G	3.7	<0.05	0.6	<0.02	0.3	<0.02	1.52	51.34	<0.1	<0.05	<0.02	<30	<20	<20	258	<20	0.02	43.0	41.9	99.4
09SZ-08-01G	4.7	<0.05	0.7	<0.02	0.4	<0.02	2.31	50.24	<0.1	<0.05	<0.02	<30	<20	<20	259	<20	0.04	41.7	41.5	99.9
09SZ-09-01G	3.4	<0.05	0.5	<0.02	0.3	<0.02	1.70	51.97	<0.1	<0.05	<0.02	<30	<20	<20	282	<20	0.07	42.8	42.0	100.0
09SZ-09-02G	5.0	<0.05	0.7	<0.02	0.3	<0.02	2.32	50.09	<0.1	<0.05	<0.02	<30	<20	<20	277	<20	0.08	41.9	41.3	99.7
09SZ-09-03G	4.0	<0.05	0.6	<0.02	0.3	<0.02	2.33	50.60	<0.1	<0.05	<0.02	<30	<20	<20	301	<20	0.05	42.2	41.9	99.8
09SZ-09-04G	4.9	<0.05	0.8	<0.02	0.4	<0.02	3.47	48.03	<0.1	<0.05	<0.02	<30	<20	<20	301	<20	0.06	42.1	41.5	99.2
09SZ-10-01G	4.2	<0.05	0.6	<0.02	0.3	<0.02	2.45	50.57	<0.1	<0.05	<0.02	<30	<20	<20	297	<20	0.08	42.2	41.7	99.9
09SZ-11-01G	5.7	<0.05	0.9	<0.02	0.4	0.02	2.78	48.49	<0.1	0.06	0.02	<30	<20	<20	304	<20	0.11	41.4	40.8	99.2
09SZ-11-02G	4.3	<0.05	0.6	<0.02	0.3	<0.02	2.63	49.66	<0.1	0.05	<0.02	<30	<20	<20	307	<20	0.06	41.9	41.8	99.4
09SZ-12-01G	4.7	<0.05	0.7	<0.02	0.3	<0.02	3.11	49.44	<0.1	<0.05	<0.02	<30	<20	<20	322	<20	0.09	42.5	41.5	99.9
09SZ-12-02G	4.6	<0.05	0.7	<0.02	0.3	<0.02	3.05	48.93	<0.1	<0.05	<0.02	<30	<20	<20	322	<20	0.06	42.2	41.6	99.3
09SZ-12-03G	4.9	<0.05	0.9	<0.02	0.4	<0.02	3.53	47.72	<0.1	0.06	<0.02	<30	<20	<20	298	<20	0.06	42.3	41.3	98.8
09SZ-13-01G	3.8	<0.05	0.9	<0.02	0.6	0.02	1.16	51.10	<0.1	0.11	0.05	<30	<20	<20	249	<20	0.19	42.3	41.3	99.0
09SZ-13-02G	2.0	<0.05	0.5	<0.02	0.3	0.02	0.95	53.56	<0.1	0.05	0.02	<30	<20	<20	279	<20	0.04	43.4	42.7	100.0
09SZ-14-01G	9.9	0.09	2.5	<0.02	0.8	0.02	2.68	44.73	<0.1	0.61	0.05	59	<20	22	286	<20	0.06	38.1	37.8	99.1
09SZ-14-02G	7.7	<0.05	1.9	<0.02	0.6	<0.02	1.88	48.13	<0.1	0.29	0.05	52	<20	<20	292	<20	0.50	39.9	39.3	100.0
09SZ-16-01G	4.8	<0.05	1.1	<0.02	0.5	0.02	1.11	51.12	<0.1	0.20	0.06	<30	<20	<20	260	<20	0.01	41.4	40.8	99.9
09SZ-17-01G	3.7	<0.05	0.6	<0.02	0.3	<0.02	2.31	50.50	<0.1	0.06	<0.02	<30	<20	<20	305	<20	0.04	42.6	41.8	99.4
09SZ-18-01G	4.0	<0.05	0.7	<0.02	0.3	<0.02	1.86	51.49	<0.1	<0.05	<0.02	<30	<20	<20	270	<20	0.02	41.9	41.8	100.3
09SZ-18-02G	4.6	<0.05	0.8	<0.02	0.4	<0.02	2.11	50.41	<0.1	0.07	<0.02	<30	<20	<20	259	<20	0.01	41.3	41.2	99.7
09SZ-18-03G	3.8	<0.05	0.6	<0.02	0.3	<0.02	1.91	51.22	<0.1	<0.05	<0.02	<30	<20	<20	265	<20	0.01	42.4	41.7	99.7
09SZ-19-01G	3.7	<0.05	0.6	<0.02	0.3	<0.02	2.00	51.39	<0.1	<0.05	<0.02	<30	<20	<20	282	<20	0.01	41.6	42.0	100.0
09SZ-20-01G	4.6	<0.05	0.9	<0.02	0.5	0.04	1.78	50.52	<0.1	0.06	<0.02	<30	<20	<20	271	<20	0.06	42.1	41.2	99.6
09SZ-20-02G	4.5	<0.05	0.7	<0.02	0.4	0.03	2.07	50.10	<0.1	0.05	<0.02	<30	<20	<20	268	<20	0.03	41.8	41.4	99.2
09SZ-20-03G	4.8	<0.05	0.8	<0.02	0.4	0.02	2.60	49.65	<0.1	0.07	<0.02	<30	<20	<20	268	<20	0.04	42.1	41.4	99.7
09SZ-20-04G	4.2	<0.05	0.7	<0.02	0.3	<0.02	2.22	50.56	<0.1	0.07	<0.02	<30	<20	<20	258	<20	0.05	41.9	41.5	99.7
09SZ-20-05G	4.4	<0.05	0.7	<0.02	0.4	<0.02	2.23	49.95	<0.1	<0.05	<0.02	<30	<20	<20	260	<20	0.04	41.3	41.6	99.3
09SZ-20-06G	3.9	<0.05	0.7	<0.02	0.3	<0.02	2.01	51.12	<0.1	0.08	<0.02	<30	<20	<20	270	<20	0.01	42.5	41.4	99.5
09SZ-21-01G	4.4	<0.05	0.9	<0.02	0.4	0.04	2.76	49.47	<0.1	0.11	<0.02	<30	<20	<20	251	<20	0.11	42.2	41.5	99.6
09SZ-03-01G_d	3.7	<0.05	0.5	<0.02	0.3	0.02	1.84	51.06	<0.1	<0.05	<0.02	<30	<20	<20	268	<20	0.07	42.2	41.8	99.4
09SZ-07-03G_d	4.5	<0.05	0.8	<0.02	0.4	<0.02	1.76	51.05	<0.1	0.07	<0.02	<30	<20	<20	260	<20	0.04	42.2	41.2	99.8
09SZ-11-02G_d	4.3	<0.05	0.6	<0.02	0.3	<0.02	2.63	49.78	<0.1	<0.05	<0.02	<30	<20	<20	306	<20	0.06	42.5	41.7	99.5
09SZ-18-01G_d	3.9	<0.05	0.6	<0.02	0.3	<0.02	1.82	50.84	<0.1	<0.05	<0.02	<30	<20	<20	268	<20	0.01	42.1	41.8	99.4

Note: 1) Fe_2O_3T is calculated value; 2) Sample Field ID with suffix _d are duplicate samples; total S and Total CO_2 are collected by LECO SC444DR Sulphur/Carbon Analyzer.

3) Classification of limestone by purity

Application of the British Geological Survey scheme for the classification of limestone by purity (Harrison, 1993; Table 6) to the XRF data (Table 5) indicates that the purity of most limestone samples from the Bad Cache Rapids and lower Churchill River groups on Southampton Island can be classified as low. Of 44 samples collected, 1 is of medium purity (54.3–52.4% CaO), 42 low purity (52.4–47.6% CaO), and 1 impure (<47.6% CaO) (Table 6). Overall, the purity is low (Fig. 8).

Table 6. Classification of limestone by purity (after Harrison, 1993) and grade of limestone on Southampton Island based on data (CaO) collected by XRF

No	Percentage of		Category	Limestone on Southmpton Island (number of samples)
	$CaCO_3$	Equivalent CaO		
1	> 98.5	> 55.2	Very high purity	0% (0/44)
2	98.5 - 97.0	55.2 - 54.3	High purity	0% (0/44)
3	97.0 - 93.5	54.3 - 52.4	Medium purity	2.3% (1/44)
4	93.5 - 85.0	52.4 - 47.6	Low purity	95% (42/44)
5	< 85.0	< 47.6	Impure	2.3% (1/44)

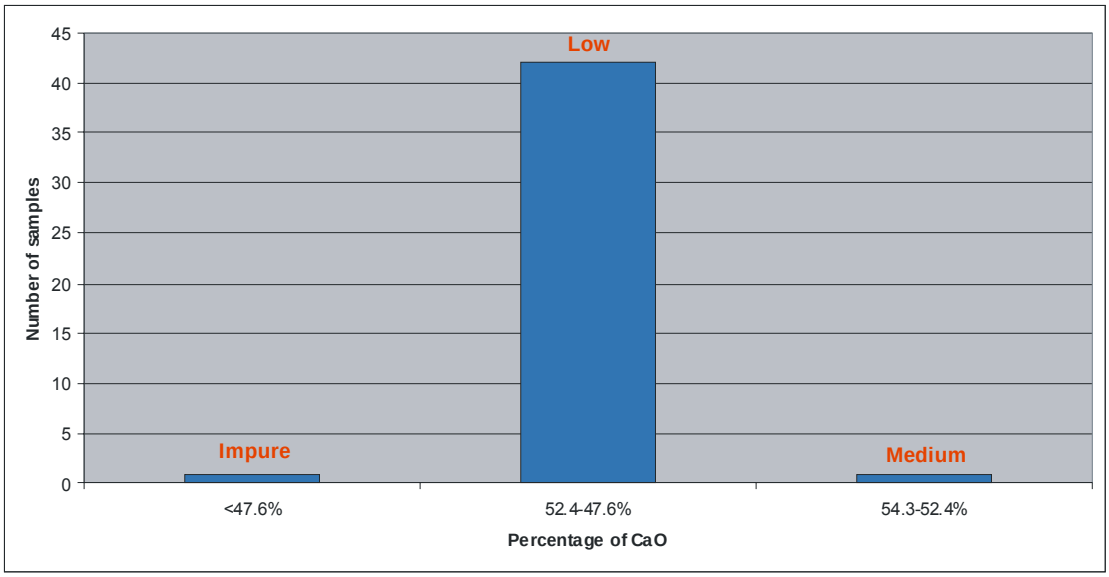

Figure 8. Classification of limestone by purity (after Harrison, 1993) on Southampton Island based on XRF data (CaO)

(3) Comparison of XRD and XRF data

As noted above, using XRD data, the Bad Cache Rapids and lower Churchill River limestones can be evaluated as medium-low purity. On the other hand, the

geochemical data derived from XRF analysis alone give a "low purity" evaluation of the same rocks. The different interpretations derived for the data from the two methodologies is reconciled below.

1) CaO (XRF) and $CaCO_3$ (XRD)

Percentage of CaO (XRF) can be converted into percentage of $CaCO_3$ by using a standard molecular weight ratio (CaO × 1.7848 = $CaCO_3$). Comparing the calculated percentage of $CaCO_3$ (XRF) with the percentage of $CaCO_3$ (XRD) (Table 7), a fairly consistent difference is apparent (Fig. 9).

The results of both XRD and XRF are most comparable for 8 samples collected from Bad Cache Rapids / Churchill River groups' boundary beds and from the base of the Rapids Group (green boxes in Fig. 9); generally these two intervals contain higher MgO. However, for 36 out of 44 samples analyzed, the percentage of $CaCO_3$ determined by XRD is higher than that calculated from the XRF data by amounts ranging from 5.6–0.87% (mean 3.14%). Two contributing factors to this bias are:

i) The percentage of $CaCO_3$ (Table 2) determined by XRD may include a small proportion of $CaMg(CO_3)_2$ (see Fig. 5); as a result, percentage of $CaCO_3$ shown in Table 2 will be modestly over-estimated.

ii) The uncertainty (<5 wt%) inherent in the XRD mineral concentration estimates (see X-ray Diffraction Analysis on p. 9) means that the bias between the XRD and XRF $CaCO_3$ estimates (mean = 3.14%) is less than the uncertainty of the measurements. However, this fails to account for the consistently higher values derived from XRD data.

Indeed, these factors are the main disadvantages of XRD outlined by Harrison et al. (1998): for conventional XRD, precision and accuracy may be poor because of overlapping peaks and differences in crystallinity and mineral chemistry between standards and samples; furthermore, detection limits are circa several percent mineral.

In general, the XRF method is a more reliable estimate of absolute abundance of elemental constituents and their oxides. For the present study, the more conservative XRF values of CaO are a better predictor for any industrial/engineering applications.

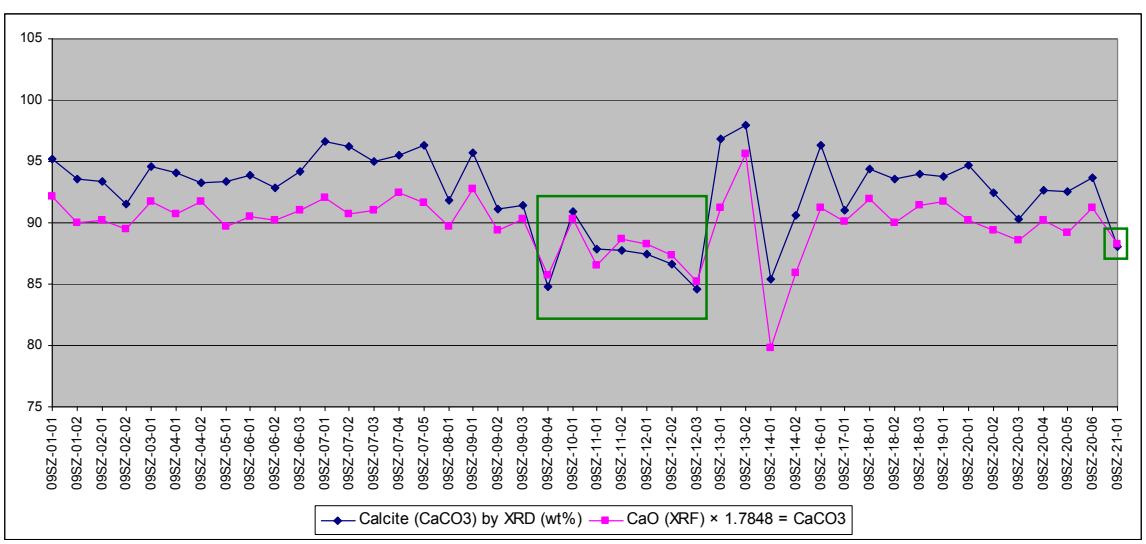

Figure 9. Comparison between XRD and XRF data.

Table 7. Comparison between $CaCO_3$ (XRD) and CaO (XRF)

Samples	Calcite ($CaCO_3$) by XRD (wt%)	Calcium oxide (CaO) by XRF (wt%)	CaO (XRF) × 1.7848 = $CaCO_3$	$CaCO_3$ (XRD) – $CaCO_3$ converted from CaO (XRF)
09SZ-01-01	95.2	51.61	92.11	3.09
09SZ-01-02	93.6	50.45	90.04	3.56
09SZ-02-01	93.4	50.55	90.22	3.18
09SZ-02-02	91.5	50.15	89.51	1.99
09SZ-03-01	94.6	51.39	91.72	2.88
09SZ-04-01	94.1	50.83	90.72	3.38
09SZ-04-02	93.3	51.39	91.72	1.58
09SZ-05-01	93.4	50.25	89.69	3.71
09SZ-06-01	93.9	50.71	90.51	3.39
09SZ-06-02	92.9	50.54	90.20	2.70
09SZ-06-03	94.2	50.98	90.99	3.21
09SZ-07-01	96.6	51.55	92.01	4.59
09SZ-07-02	96.2	50.82	90.70	5.50
09SZ-07-03	95	50.98	90.99	4.01
09SZ-07-04	95.5	51.78	92.42	3.08
09SZ-07-05	96.3	51.34	91.63	4.67
09SZ-08-01	91.8	50.24	89.67	2.13
09SZ-09-01	95.7	51.97	92.76	2.94
09SZ-09-02	91.1	50.09	89.40	1.70
09SZ-09-03	91.4	50.60	90.31	1.09
09SZ-09-04	84.8	48.03	85.72	-0.92
09SZ-10-01	90.9	50.57	90.26	0.64
09SZ-11-01	87.9	48.49	86.54	1.36
09SZ-11-02	87.8	49.66	88.63	-0.83
09SZ-12-01	87.4	49.44	88.24	-0.84
09SZ-12-02	86.6	48.93	87.33	-0.73
09SZ-12-03	84.6	47.72	85.17	-0.57
09SZ-13-01	96.8	51.10	91.20	5.60
09SZ-13-02	98	53.56	95.59	2.41
09SZ-14-01	85.4	44.73	79.83	5.57
09SZ-14-02	90.6	48.13	85.90	4.70
09SZ-16-01	96.3	51.12	91.24	5.06
09SZ-17-01	91	50.50	90.13	0.87
09SZ-18-01	94.4	51.49	91.90	2.50
09SZ-18-02	93.6	50.41	89.97	3.63
09SZ-18-03	94	51.22	91.42	2.58
09SZ-19-01	93.8	51.39	91.72	2.08
09SZ-20-01	94.7	50.52	90.17	4.53
09SZ-20-02	92.5	50.10	89.42	3.08
09SZ-20-03	90.3	49.65	88.62	1.68
09SZ-20-04	92.7	50.56	90.24	2.46
09SZ-20-05	92.6	49.95	89.15	3.45
09SZ-20-06	93.7	51.12	91.24	2.46
09SZ-21-01	88.1	49.47	88.29	-0.19

2) SiO_2 (XRF) and SiO_2 (XRD)

SiO_2 is an oxide that can be determined by XRF; on the other hand, quartz is a mineral that can be analyzed by XRD. However, XRF provided higher percentages of SiO_2 (2.0-9.9%) than did XRD (1.2-6.2%) for all the 44 samples (Table 8; Fig. 10); on average, the percentage of SiO_2 (XRF) is 1.38% higher than that of SiO_2 (XRD). This minor discrepancy may simply be a function of the high determination limit and analytical error of XRD analysis.

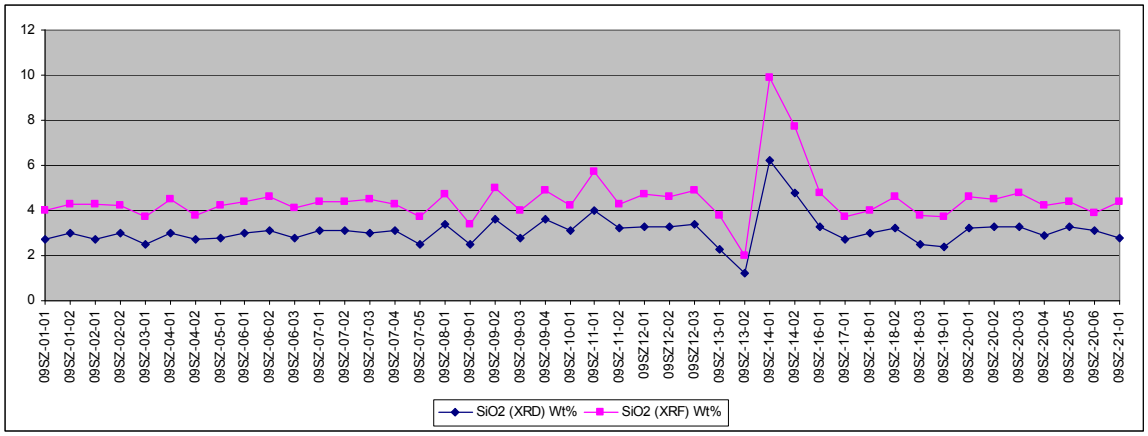

Figure 10. Comparison between SiO2 (XRD) and SiO2 (XRD)

Table 8. Comparison between SiO_2 (XRD) and SiO_2 (XRF)

Samples	SiO_2 (XRD) Wt%	SiO_2 (XRF) Wt%	Difference between SiO_2 (XRD) and SiO_2 (XRF)
09SZ-01-01	2.7	4.0	-1.3
09SZ-01-02	3	4.3	-1.3
09SZ-02-01	2.7	4.3	-1.6
09SZ-02-02	3	4.2	-1.2
09SZ-03-01	2.5	3.7	-1.2
09SZ-04-01	3	4.5	-1.5
09SZ-04-02	2.7	3.8	-1.1
09SZ-05-01	2.8	4.2	-1.4
09SZ-06-01	3	4.4	-1.4
09SZ-06-02	3.1	4.6	-1.5
09SZ-06-03	2.8	4.1	-1.3
09SZ-07-01	3.1	4.4	-1.3
09SZ-07-02	3.1	4.4	-1.3
09SZ-07-03	3	4.5	-1.5
09SZ-07-04	3.1	4.3	-1.2
09SZ-07-05	2.5	3.7	-1.2
09SZ-08-01	3.4	4.7	-1.3
09SZ-09-01	2.5	3.4	-0.9
09SZ-09-02	3.6	5.0	-1.4
09SZ-09-03	2.8	4.0	-1.2
09SZ-09-04	3.6	4.9	-1.3
09SZ-10-01	3.1	4.2	-1.1
09SZ-11-01	4	5.7	-1.7
09SZ-11-02	3.2	4.3	-1.1
09SZ12-01	3.3	4.7	-1.4
09SZ12-02	3.3	4.6	-1.3
09SZ12-03	3.4	4.9	-1.5
09SZ-13-01	2.3	3.8	-1.5
09SZ-13-02	1.2	2.0	-0.8
09SZ-14-01	6.2	9.9	-3.7
09SZ-14-02	4.8	7.7	-2.9
09SZ-16-01	3.3	4.8	-1.5
09SZ-17-01	2.7	3.7	-1.0
09SZ-18-01	3	4.0	-1.0
09SZ-18-02	3.2	4.6	-1.4
09SZ-18-03	2.5	3.8	-1.3
09SZ-19-01	2.4	3.7	-1.3
09SZ-20-01	3.2	4.6	-1.4
09SZ-20-02	3.3	4.5	-1.2
09SZ-20-03	3.3	4.8	-1.5
09SZ-20-04	2.9	4.2	-1.3
09SZ-20-05	3.3	4.4	-1.1
09SZ-20-06	3.1	3.9	-0.8
09SZ-21-01	2.8	4.4	-1.6

6. PETROGRAPHIC ANALYSIS

The main purpose of a petrographic (thin-section) analysis is to evaluate the bulk mineralogy and link the results of whole rock geochemical analysis and field observation. The thin sections provide important textural information about the localized occurrence of trace or minor impurities in the limestones. For example, dolomite, clay minerals and diagenetic iron (e.g. pyrite) will commonly form under particular localized conditions.

Thin-sections of a total of 39 samples were made by Calgary Rock and Materials Services Inc. They are routinely prepared by impregnating rock samples with blue epoxy to identify porosity and to prevent delicate structures (e.g. clays) from being destroyed during preparation. Two samples (09SZ-12-02 and 09SZ-20-04) were stained with alizarin red S to distinguish calcite from dolomite, and with potassium ferricyanide to distinguish ferroan carbonate, if present.

(1) Mineralogy

Calcite accounts for the majority of the total rock composition with minor dolomite and quartz in all the samples. Clay minerals were also noted in these rocks.

1) Calcite

Calcite is easily identified by the light red coloration it displays in plane light due to staining. Calcite commonly displays pastel interference colors in cross-polarized light, but occasionally the interference colors are more vibrant where crystal size is small or the section is slightly thinner than the standard 30µm. The majority of the calcite which composes the matrix is microcrystalline calcite (i.e. micrite), which makes up the brown area in Figs. 10 and 11. Individual crystals are indistinguishable and the micrite often has a dark appearance.

Minor blocky calcite cement is observed, which likely has a burial origin. Some of the cavities may be attributed to primary porosity, but others are clearly moulds created by leaching of susceptible fragments (e.g. Fig. 14, image C and D, D-5 to F-8). These moulds occasionally have preserved micritic envelopes that illustrate the outer extent of the former bioclastic fragment. The crystal size of the cement increases toward the center of the cavities from microspar (4-10µm) to sparry calcite (maximum size 0.6mm).

2) Dolomite

Overall, dolomites are concentrated in irregular zones with higher porosity (greenish blue zones due to higher porosity and epoxy in Figs. 10 and 11). On an outcrop scale, these zones can be observed on bedding planes as irregular and continuous zones (~ 0.5–1 cm wide) of yellowish-orange mottling (Figs. 3 and 12). These meandering zones are typical of bioturbation structures that dolomitization commonly follows.

Dolomite is observed as colorless, coarse silt-sized rhombs (30-50µm) with occasional rhombs observed up to very-fine crystalline (100-125µm). The dolomite tends to be uniform-sized euhedral crystals in the samples from lower Churchill River Group (Fig. 13), and euhedral with minor subhedral crystals in almost all samples from the Bad Cache

Rapids Group (Fig. 14). The majority of the dolomite is observed within the irregular zones (Fig. 13A, 13B, 14B-14D), but occasional isolated rhombs or small patches of dolomite rhombs are also observed dispersed throughout the matrix. Typically, the porosity is higher in dolomite-rich zones than in calcite-rich areas. It is easy to observe that the dolomite crystals "invade" into the bioclastic fragments and other grains from their edges (e.g., Fig. 12). This is an indication that the dolomitization is secondary, which agrees with the bulk result from X-ray diffraction analysis.

3) Rough visual estimation of $CaCO_3$ percentage

In order to test which geochemical data set, XRD or XRF, provides more reliable $CaCO_3$ content estimates, a rough visual estimation of $CaCO_3$ percentage was performed using thin sections.

As shown in Fig. 10 and 11, dolomites are concentrated in the greenish blue porous irregular zones. Taking sample 09SZ-20-04 (Fig. 11) as an example and neglecting SiO_2 and other trace minerals, a rough estimation of $CaCO_3$ percentage can be done as follows:

i) $\sum CaCO_3$-dominated area = $\sum$area of thin section – $\sum$area of $MgCO_3$-dominated zones;

ii) $\sum CaCO_3$ weight = $\sum CaCO_3$-dominated area × $CaCO_3$ molecular weight (100.0869);

iii) $\sum MgCO_3$ weight = $\sum MgCO_3$-dominated area × $MgCO_3$ molecular weight (84.3139);

iv) percentage of $CaCO_3$ = $\sum CaCO_3$ weight / ($\sum CaCO_3$ weight + $\sum MgCO_3$ weight)

Therefore, the percentage of $CaCO_3$-dominated area in thin section 9SZ-20-04 is 81.5%, and the estimated percentage weight of $CaCO_3$ is about 84%. This rough estimation of $CaCO_3$ percentage is lower than the percentage provided by both XRD (92.7%) and XRF (90.24%; converted), but closer to that of XRF than that of XRD.

4) Quartz/chert (silica)

Quartz/chert is colorless in plane light, but is easily distinguished from dolomite due to the lack of inclusions giving quartz a brighter appearance in plane light than exhibited by dolomite. These minerals also have distinctly different forms in these samples since the chert is present as patchy or complete replacement of bioclasts (Fig. 14C and 14D, O-3 to R-7). In cross-polarized light, chert will often display very low (first-order grey) interference colors which makes it easy to distinguish from dolomite which displays similar interference colors to calcite.

5) Questionable mineral

Phosphate might be present as a secondary mineral (Fig. 15A, G4-M4). The "phosphate" crystals are dark yellow to brown, and often found concentrated in clusters or rimming carbonate bioclasts (dark area in Fig. 15D). However, XRF detected less than 0.02% P_2O_5 (Table 5) for most of the samples; thus it is questionable whether these dark minerals are phosphate.

Figure 10. Overview of thin section, with blue epoxy, of sample 09SZ-12-02 from the lower Churchill River Group. Note the presence of irregular patches of diagenetic dolomite (greenish blue zones). Arrow indicates stratigraphic orientation (up direction).

Figure 11. Overview of thin section, with blue epoxy, of sample 09SZ-20-04 from the lower Bad Cache Rapids Group. Note the presence of irregular patches of diagenetic dolomite (greenish blue zones). Arrow indicates stratigraphic orientation (up direction).

Figure 12. Typical mottling (=patchy dolomite) on a bedding plane of Bad Cache Rapids Group limestone at Fossil Creek.

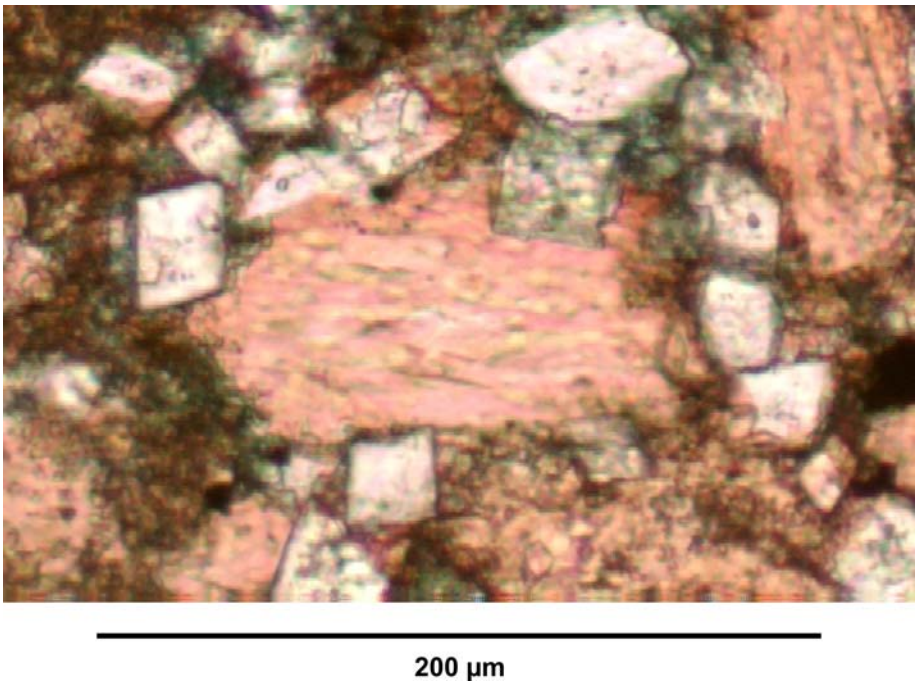

Figure 13. Secondary dolomitization observed in thin section 09SZ-12-02 from the lower Churchill River Group.

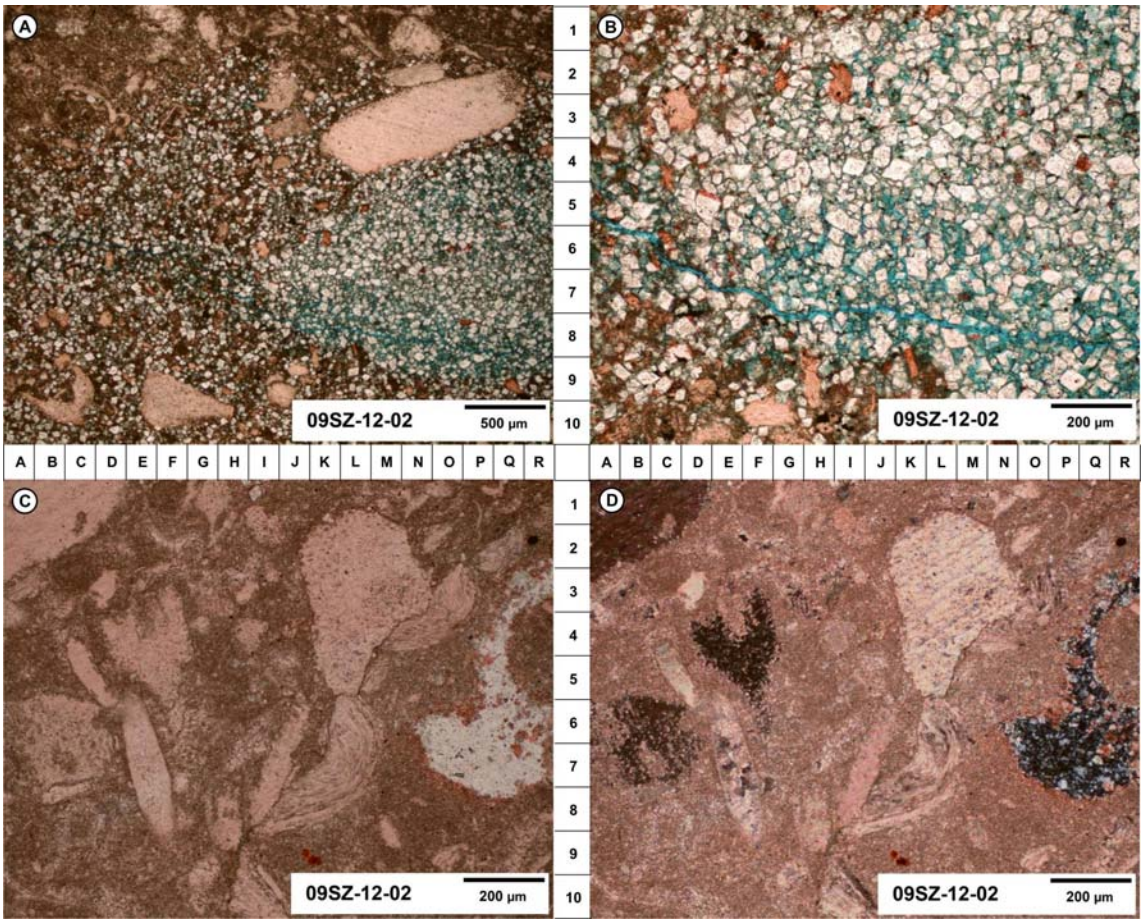

Figure 14. Detailed thin section views of sample 09SZ-12-02 (lower Churchill River Group).

A. transition between a predominantly calcitic matrix and a significantly dolomitized zone. Note the dolomite rhombs (colorless) are generally uniform in size.

B. higher magnification view of A.

C. a variety of calcitic bioclasts in a matrix composed of micrite to microspar. The bioclasts in this view are predominantly echinoderm fragments (crinoids and/or blastoids). A pressure solution seam can be observed starting at I-10 to R-1 defined by the abrupt terminations of different adjacent bioclasts. Note the colorless fragment located at O-3 to R-7 which is a bioclast that has been replaced by chert.

D. same view as A, but in cross-polarized light.

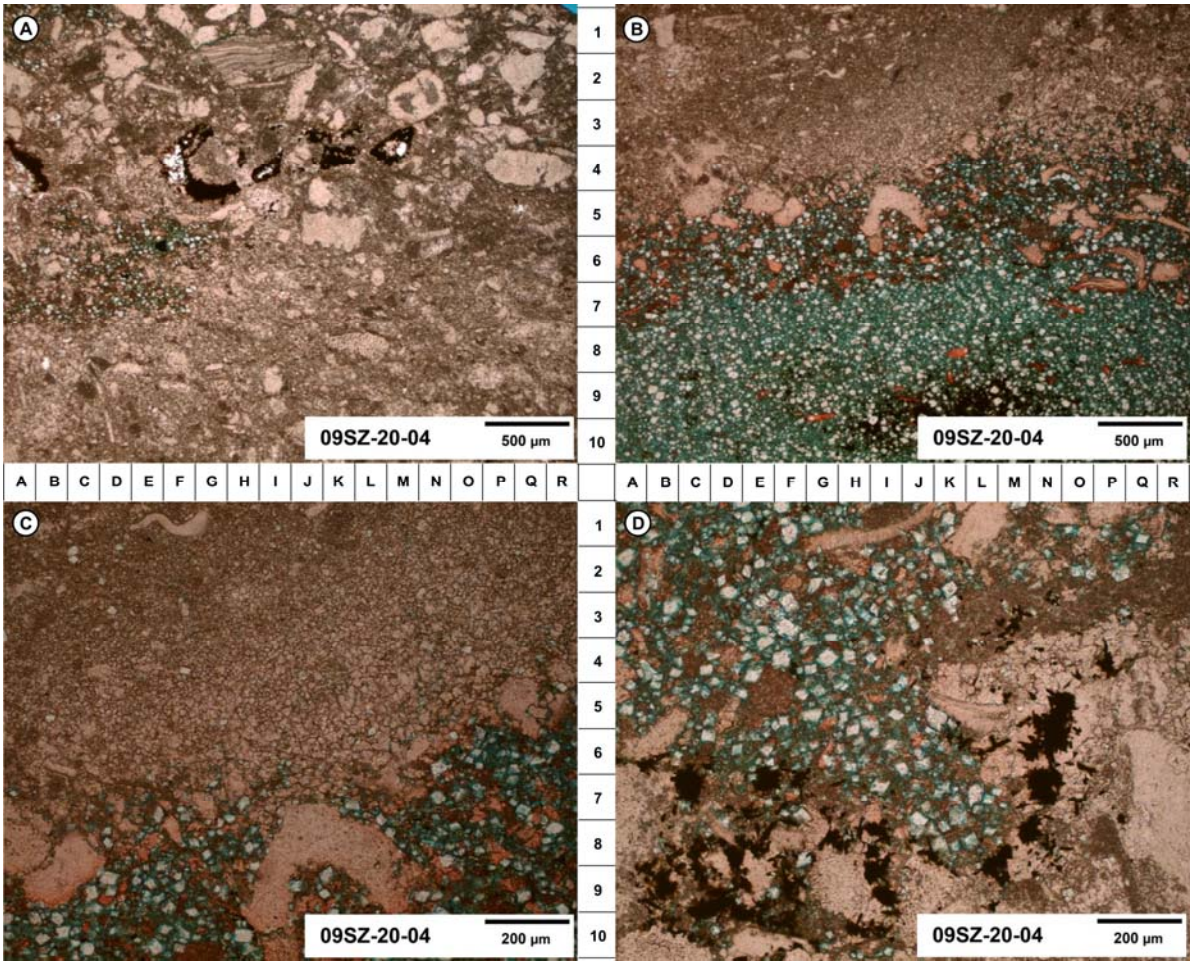

Figure 15. Detailed thin section views of sample 09SZ-20-04 (lower Bad Cache Rapids Group).

A. abundance of bioclastic fragments in a matrix that is more micritic toward the upper part of the image, and more microspar/pseudospar toward the bottom of the image. Note that the preservation of the bioclastic fragments appears better in the more micritic area, implying the microspar area has been subjected to more significant diagenesis. The dark areas in the image (e.g. G-4) are clusters of phosphate crystals.

B. gradational trend (downwards) from a predominantly micritic matrix through microspar, pseudospar and finally to dolomitic zones.

C. higher magnification view of part of B; dolomitic zone front.

D. area with common patches of "phosphate" crystals that commonly rim bioclastic fragments.

(2) Rock Fabric

Based on thin section analysis, most of the samples collected by this study can be defined as dolomitic wackestone-packstone using Dunham's (1962) classification modified by Embry and Klovan (1971).

The limestone contains abundant bioclasts that are largely mud-supported to matrix-supported (wackestone), but grain-supported areas (packstone) are also common. The majority of the bioclasts (Figs. 9 and 10) are less than 2mm in diameter, although a small percent exceed 2mm. The bioclasts contain a variety of different fragments including echinoid fragments (the majority of which are crinoids), bryozoans, ostracodes, molluscs (bivalves), sponges, corals and foraminifera. Diagenesis has had a significant impact on the rock. It has obscured some of the detail of the bioclasts and has altered the

primary depositional textures, primarily due to recrystallization of the matrix and selective dolomitization.

The matrix is dominated by micrite trending through microspar (4-10µm) and pseudospar (10-50µm). Often, the area beyond the pseudospar has been dolomitized. This gradational increase in crystal size is best observed in Fig. 14A and 14B. Fractures are minor in these samples but, when observed, they most often occur in the dolomitic zones and through the calcitic matrix often connecting the dolomitic zones. Microfractures are also noted along the rims of larger bioclastic fragments. Pressure solution seams are occasionally noted; an abrupt termination observed in a bioclastic fragment can be traced through adjacent bioclasts where a pressure solution seam is present (Fig. 14C, I-10 to R-1).

Close examination of the matrix shows general micro-heterogeneity throughout the rock with alternating micrite and microspar. This indicates that originally the rocks may have contained abundant microfossils that have now been obscured due to diagenetic alteration.

7. Conclusions and Possible Subsequent Work

Limestone exposures over Rocky Brook, the coastal area east of Rocky Brook, Fossil Creek and vicinity, and east of Post River on Southampton Island belong to the Upper Ordovician Bad Cache Rapids Group and lower Churchill River Group. The following conclusions are based on the geochemical analyses for 44 samples and petrographic and field observations in these areas.

(1) Conclusions

- Multiple analytical techniques were employed to assess limestone quality/geochemistry. X-Ray Fluorescence (XRF) provides the most reliable absolute value data for major oxides (e.g. CaO) and elements. Overall, the limestones around Coral Harbour (Bad Cache Rapids and lower Churchill River groups) predominantly demonstrate chemical-industrial purity value of “Low Purity”.
- Limestones of comparable (low) purity are conventionally used in non-chemically dependant applications, such as aggregate sources. Small volumes of the Bad Cache Rapids limestone are currently being used in Coral Harbour as road-building material.
- Study sites included areas of known significant thickness, within reasonable (i.e. exploitable) distance of Coral Harbour. Of these, the area around Fossil Creek (site 3) contains the least continuous volume of limestones, and is least likely for development, owing to existing recreational and transportation use. Rocky Brook (site 1) contains one of the thickest continuous sections of limestones: while the river course itself is unsuitable for excavation, large areas inland preserve the same strata, currently unexposed. A large Paleozoic limestone outlier east of the Post River (site 4) preserves the full thickness of Bad Cache Rapids Group, and would

present the least environmental challenge for possible excavation/development. A large area of raised beach, east of Rocky Brook (site 2), contains mixed-provenance limestone rubble, and could be suitable for shallow stripping.

(2) Possible Subsequent Work

1) Discussion

An important manufactured lime product, calcine or quick-lime (CaO), will be required for Kivalliq mines in Nunavut. Calcine is produced from high-calcite ($CaCO_3$) limestone, in a reduction to CaO normally achieved through kiln-firing. The input limestone requirements for calcination are amongst the more stringent for the industrial applications. A high to very high purity is required (>97% $CaCO_3$). In nature, beds of limestone of this purity occur quite rarely. In a typical commercial quarry, these high-$CaCO_3$ intervals are normally confined to a few meters thickness, with the other beds suitable for less demanding uses, or stripped as aggregate or even waste. High-$CaCO_3$ beds require special geological conditions in which to form. These may be: chemical precipitation from seawater (evaporitic limestone); preservation of pure lime mud (micrite or marl), with negligible chemical alteration post-burial; pure reef limestone, consisting of large frame-building fossils.

A thorough examination of limestone exposures around Coral Harbour has revealed the absence of any sedimentologically distinct high-grade beds of intervals (except for one sample). Indeed, the Bad Cache Rapids limestone around Coral Harbour exhibit the characteristics of a typical detrital limestone, a moderately washed (at time of deposition) mixture of organically-derived lime particles and muds. Indeed, the hallmark of these rocks locally is their extreme homogeneity – there is little compositional variation, bed to bed. There is nothing in the exposed beds to suggest higher-grade variations exist laterally nearby, under cover.

Therefore, follow-up studies aimed at sourcing higher purity limestone should expand the stratigraphical and geographical coverage of this study.

2) Reasonable potentials

- Stratigraphically moving upwards to test the beds within upper Churchill River Group of the Upper Ordovician and the Severn River and Ekwan River formations of the Lower Silurian on Southampton Island, especially the two Lower Silurian units. The chemical analyses of samples collected from the Ekwan River and Attawapiskat formations in Moose River Basin (northern Ontario) indicate the potential for high-calcium limestone with $CaCO_3$ ranging 96.86–97.40% in the Ekwan River Formation and 98.03–100% in the Attawapiskat Formation (Kelly, 1996). These two formations were almost equally developed in both Moose River and Hudson Bay basins during the Early Silurian.
- Geographically expanding the study to areas on the eastern Melville Peninsula, where the Bad Cache Rapids Group-equivalent limestone is well exposed, and on southern Baffin Island, where the Bad Cache Rapids and Churchill River groups-equivalent limestones occur. Previous work in these areas, though superficial, suggests the possibility that intervals of higher calcite purity might be present.

Acknowledgements

Financial support provided by Strategic Investments in Northern Economic Development (SINED), Canadian Northern Economic Development Agency, is acknowledged. Critical reviews of Drs. S. Jackson (GSC, Ottawa) and F. Brunton (Ontario Geological Survey) are greatly appreciated. Field assistance was provided by Coral Harbor Hunters and Trappers Organization.

References

Dunham, R.J. 1962: Classification of carbonate rocks according to depositional texture. In: Ham, W.E. (Ed.), Classification of Carbonate rocks. American Association of Petroleum Geologists Memoir 1, Tulsa, Oklahoma, pp. 108-121.

Embry, A.F., and Klovan, J.E. 1971: A Late Devonian reef tract on Northeastern Banks Island, NWT: Canadian Petroleum Geology Bulletin, v. 19, p. 730-781.

Harrison, D.J. 1992: High-purity limestones in England and Wales. Quarterly Journal of Engineering Geology, 26, 293-303.

Harrison, D.J., Inglethorpe, S.D.J., Mitchell, C.J., Kemp, S.J., Chaodumrong, P., and Charusribandhu, M. 1998: Procedures for the rapid assessment of limestone resources. British Geological Survey Technical Report WC/98/1, 120pp.

Heywood, W.W., and Sanford, B.V., 1976: Geology of Southampton, Coats and Mansel Islands, District of Keewatin, Northwest Territories. Geological Survey of Canada, Memoir 382, 35p.

Kelly, R.I. 1996: High-purity calcite and dolomite resource of Ontario. Ontario Geological Survey, Open File Report 5954, 39 pp.

Zhang, S. 2008: New insight into Ordovician oil shales in Hudson Bay: their number, stratigraphic position, and petroleum potential. Bulletin of Canadian Petroleum Geology, v. 56, p. 300–324.

Zhang, S. 2011: Late Ordovician conodont biostratigraphy and redefinition of the age of oil shale intervals on Southampton Island. Canadian Journal of Earth Sciences, v. 48, p. 619-643.

Zhang, S., and Barnes, C.R. 2007: Late Ordovician–Early Silurian Conodont Biostratigraphy and Thermal Maturity, Hudson Bay Basin. Bulletin of Canadian Petroleum Geology, v. 55, p. 179–216.